Drug Design, Development and Therapy

ISSN: (Print) (Online) Journal homepage: informahealthcare.com/journals/dddt20

Design, synthesis, and antitumor evaluation of histone deacetylase inhibitors with l-phenylglycine scaffold

Yingjie Zhang, Xiaoguang Li, Jinning Hou, Yongxue Huang & Wenfang Xu

To cite this article: Yingjie Zhang, Xiaoguang Li, Jinning Hou, Yongxue Huang & Wenfang Xu (2015) Design, synthesis, and antitumor evaluation of histone deacetylase inhibitors with l-phenylglycine scaffold, Drug Design, Development and Therapy, , 5553-5567, DOI: 10.2147/DDDT.S94037

To link to this article: https://doi.org/10.2147/DDDT.S94037

Published online: 08 Oct 2015.

Drug Design, Development and Therapy

Dovepress
open access to scientific and medical research

Open Access Full Text Article

ORIGINAL RESEARCH

Design, synthesis, and antitumor evaluation of histone deacetylase inhibitors with L-phenylglycine scaffold

This article was published in the following Dove Press journal:
Drug Design, Development and Therapy
8 October 2015
Number of times this article has been viewed

Yingjie Zhang[1]
Xiaoguang Li[1]
Jinning Hou[1]
Yongxue Huang[2]
Wenfang Xu[1]

[1]Department of Medicinal Chemistry, School of Pharmacy, Shandong University, Ji'nan, [2]Weifang Bochuang International Biological Medicinal Institute, Weifang, Shandong, People's Republic of China

Abstract: In our previous research, a novel series of histone deacetylase (HDAC) inhibitors with L-phenylglycine scaffold were designed and synthesized, among which amides **D3** and **D7** and ureido **D18** were far superior to the positive control (suberoylanilide hydroxamic acid [SAHA]) in HDAC inhibition, but were only comparable to SAHA in antiproliferation on tumor cell lines. Herein, further structural derivation of lead compounds **D3**, **D7**, and **D18** was carried out to improve their cellular activities. Most of our newly synthesized compounds exhibited more potent HDAC inhibitory activities than the positive control SAHA, and several derivatives were even better than their parent compounds. However, compared with SAHA and our lead compounds, only secondary amine series compounds exhibited improved antiproliferative activities, likely due to their appropriate topological polar surface area values and cell permeabilities. In a human histiocytic lymphoma (U937) xenograft model, the most potent secondary amine **9d** exhibited similar in vivo antitumor activity to that of SAHA.

Keywords: phenylglycine, histone deacetylases, inhibitor, antitumor

Introduction

Research and development of antitumor drugs targeting epigenetic mechanism has become a hot topic in the field of antitumor therapy. Among the epigenetics-related enzymes, histone deacetylases (HDACs) are drawing more and more attention from the academic community and the pharmaceutical industry because aberrant deacetylation of nucleosomal histone and other nonhistone substrates is closely related to tumorigenesis and because many HDAC inhibitors used alone or combined with other antitumor drugs demonstrate promising results in preclinical research and clinical trials.[1–3]

HDAC inhibitors could induce different phenotypes in various transformed cells, including cell-cycle arrest, mitotic cell death and senescence, autophagic cell death, activation of the extrinsic and/or intrinsic apoptotic pathways, DNA damage and oxidative stress, antiangiogenesis, disruption of chaperone function, etc.[4,5]

Currently, four HDAC inhibitors, including suberoylanilide hydroxamic acid (SAHA), FK228, PXD101, and LBH589 were approved by the US Food and Drug Administration, and one HDAC inhibitor CS005 was approved by the China Food and Drug Administration for cancer treatment (Figure 1A). Besides, approximately 20 small molecular HDAC inhibitors are in different phases of clinical trials (Figure 1B). It is worth noting that from the end of 2014 to the beginning of 2015, there were three HDAC inhibitors consecutively approved, which indicates the rapid development in the research field of HDACs and HDAC inhibitors.

Correspondence: Yingjie Zhang; Wenfang Xu
Department of Medicinal Chemistry, School of Pharmacy, Shandong University, Ji'nan, Shandong 250012, People's Republic of China
Tel/fax +86 531 8838 2009; +86 531 8838 2264
Email zhangyingjie@sdu.edu.cn; wenfxu@163.com

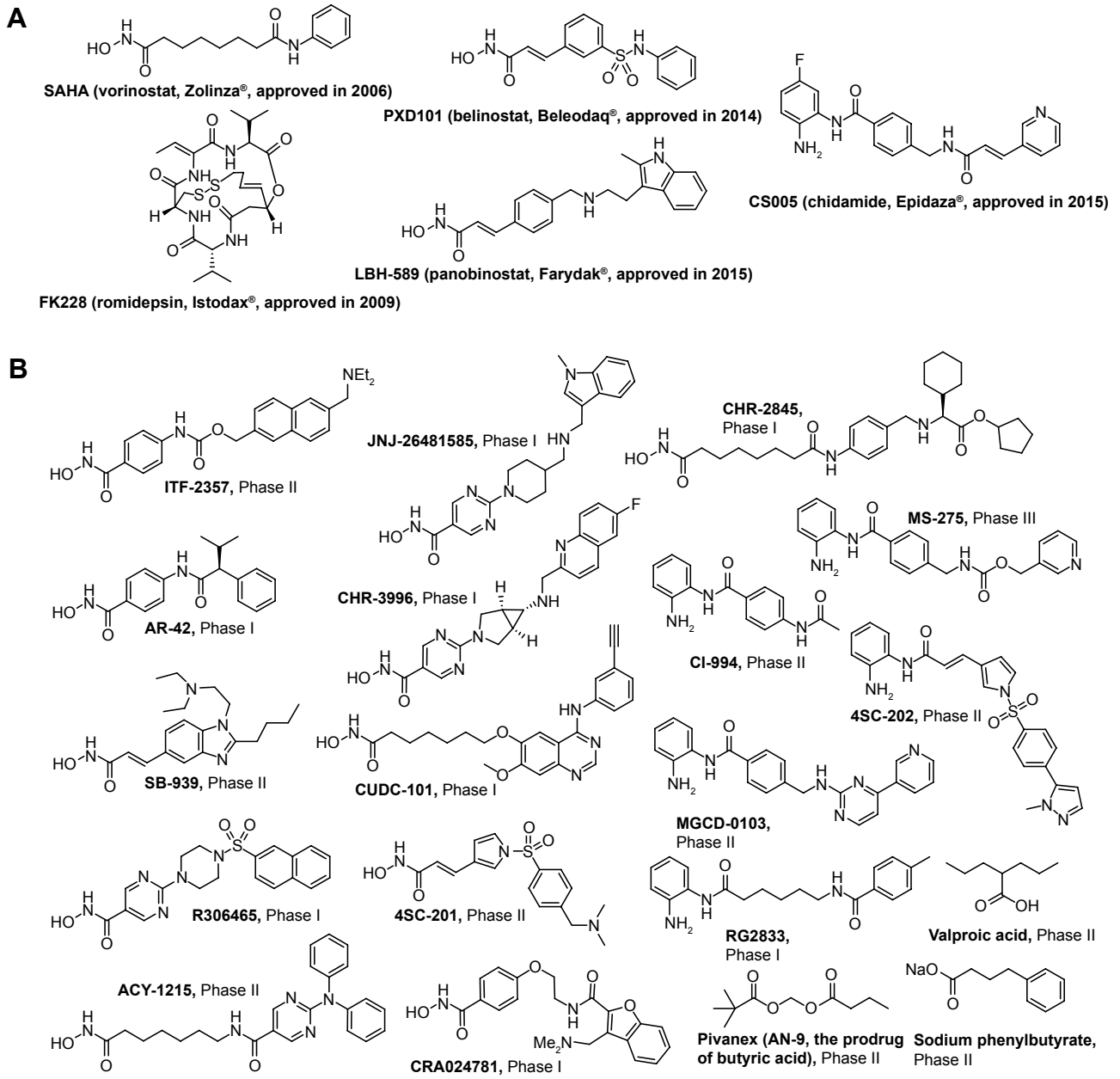

Figure 1 The structures of five approved drugs (**A**) and HDAC inhibitors in clinical trials (**B**).
Abbreviations: SAHA, suberoylanilide hydroxamic acid; HDAC, histone deacetylase.

In order to find potent HDAC inhibitors, a virtual screening approach was performed in our lab, and we discovered a hit compound **1** (Figure 2).[6] Structural modification and derivation of this hit compound generated a novel series of phenylglycine-based hydroxamic acids with potent HDAC inhibitory activity and antitumor potency.[7,8] The general structure of these phenylglycine-based hydroxamic acids are represented in structure **2** (Figure 2). Although most of our previously discovered phenylglycine-based HDAC inhibitors exhibited more potent HDAC inhibitory activities than the approved drug SAHA, their in vitro antiproliferative potency was just similar to that of SAHA.[8] Therefore, based on our previous lead compounds **D18**, **D3**, and **D7**,[8] the main purpose of this work was to find HDAC inhibitors with more satisfying antiproliferative potency. Our compound design strategy mainly focused on the following three aspects (Figure 2).

First, in our previous work, only two ureido analogs were synthesized and one of them, **D18** exhibited approximately 20-fold more potent HDAC inhibition than the approved drug SAHA.[8] In this work, comprehensive structure–activity relationship study of **D18** was performed to develop ureido analogs with improved activity.

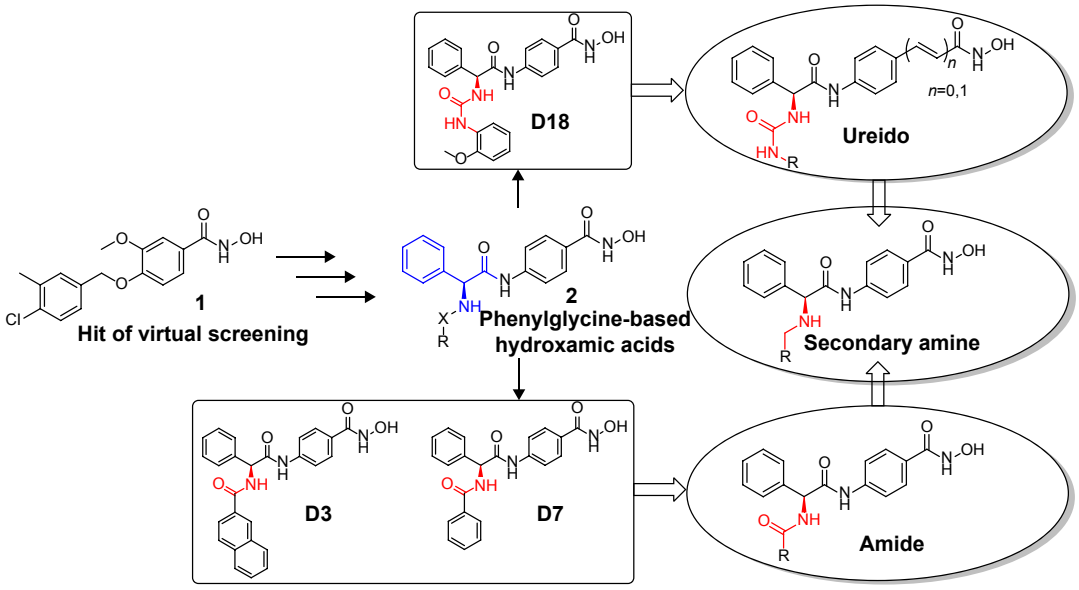

Figure 2 The development of phenylglycine-based HDAC inhibitors.
Abbreviation: HDAC, histone deacetylase.

Second, the naphthyl group of **D3** and phenyl group of **D7** were replaced with several aromatic heterocycles to fine-tune their partition coefficient. We hope that introduction of nitrogen atoms could improve the water solubility and antiproliferative potency of **D3** and **D17**.

Finally, considering that the antiproliferative potency of HDAC inhibitor is largely determined by their cell permeability, which is closely related to the topological polar surface area (tPSA) value,[9] a series of secondary amine analogs were designed and synthesized, which should have preferable tPSA values due to their fewer polar atoms than the ureido and amide compounds.

Experimental materials and methods

Unless specified otherwise, all starting materials, reagents, and solvents were commercially available. All reactions except those in aqueous media were carried out by standard techniques for the exclusion of moisture. All reactions were monitored by thin-layer chromatography (TLC) on 0.25 mm silica gel plates (60GF-254) and visualized with ultraviolet light, ferric chloride, or iodine vapor. Nuclear magnetic resonance (NMR) spectra were determined using Bruker DRX or Varian INOVA spectrometers, chemical shift (δ) in parts per million and coupling constant (J) in hertz, using tetramethylsilane as an internal standard. Measurements were made in dimethyl sulfoxide (DMSO)-d_6 solutions. Electrospray ionization–mass spectroscopy (ESI–MS) was carried out using an API 4000 spectrometer (MDS SCIEX, Concord, ON, Canada). High-resolution mass spectroscopy (HRMS) was conducted by Shandong Analysis and Test Center (Jinan, Shandong, People's Republic of China). Silica gel was used for column chromatography purification. Melting points (Mps) were determined using an electrothermal Mp apparatus and were uncorrected.

Chemistry

The ureido compounds **7a**–**7k**, amide compounds **8a**–**8e**, and secondary amine compounds **9a**–**9g** were synthesized according to the procedures described in Figure 3. The starting material, compound **3**, was obtained according to our methods published in our previous study.[8] Different kinds of aromatic amines were treated with triphosgene [bis(trichloromethyl) carbonate] to get corresponding isocyanates, and subsequently, the reaction of obtained isocyanates with compound **3** in the presence of Et_3N afforded intermediates **4a**–**4k**, which were treated with NH_2OK in methanol to get target compounds **7a**–**7k**. The starting material **3** was condensed with carboxylic acids or aldehydes to get intermediates **5a**–**5e** and **6a**–**6g**, respectively, which were finally transformed into target hydroxamate compounds **8a**–**8e** and **9a**–**9g**.

Target compounds **16a**–**16d** were synthesized using the procedures described in Figure 4. Methyl ester protection and subsequent reduction of compound **10** provided intermediate **11**. Condensation of **11** with Boc-phenylglycine **12**, N-deprotection, followed by reaction with isocyanates led to compounds **15a**–**15d**. The ester groups of **15a**–**15d** were treated with NH_2OK to get target compounds **16a**–**16b**.

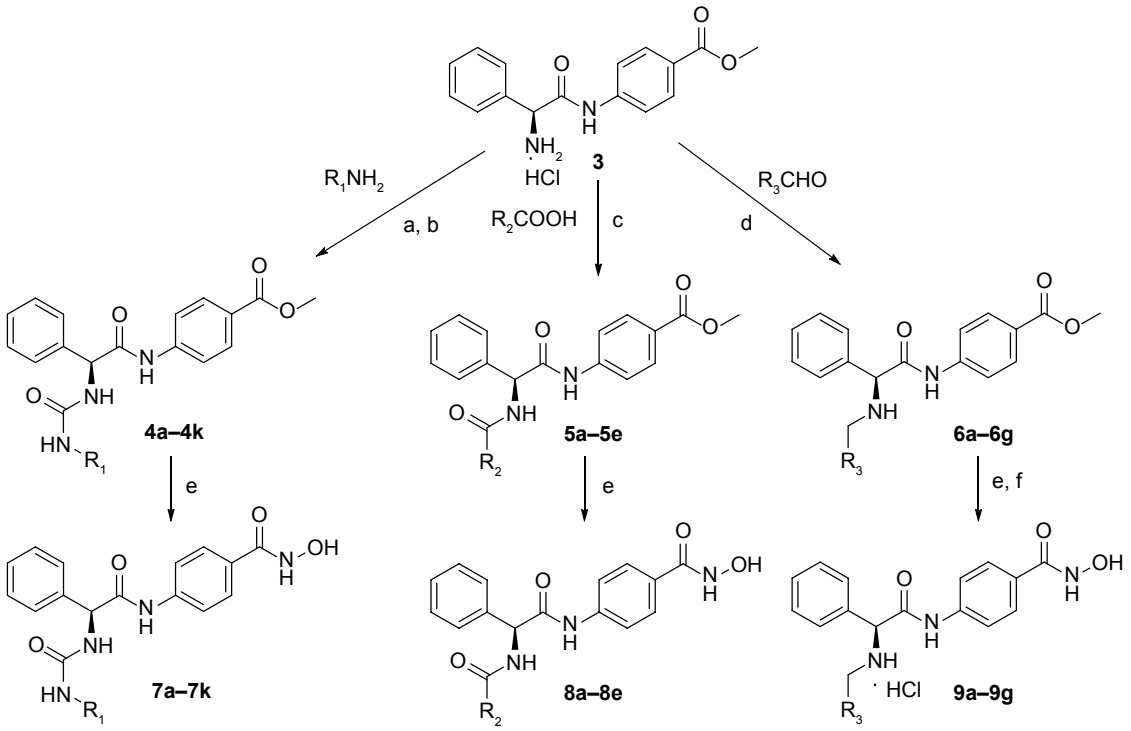

Figure 3 Reagents and conditions: (a) BTC, dioxane, reflux; (b) Et_3N, DCM; (c) TBTU, Et_3N, DCM; (d) $NaBH_3(CN)$, AcOH, EtOH; (e) NH_2OK, MeOH; (f) HCl, anhydrous EtOAc.
Abbreviations: BTC, bis(trichloromethyl) carbonate; DCM, dichloromethane; TBTU, 2-(1*H*-benzotriazole-1-yl)-1,1,3,3-tetramethyluronium tetrafluoroborate.

Methyl (*S*)-4-(2-amino-2-phenylacetamido) benzoate hydrochloride (3)

Compound **3** was synthesized according to the methods described in our previous study.[8]

Methyl (*S*)-4-(2-(3-(3-methoxyphenyl) ureido)-2-phenylacetamido)benzoate (4a)

At 0°C, 3-methoxyaniline (1.23 g, 10 mmol) was added to a solution of triphosgene (1.50 g, 5.0 mmol) in dioxane (50 mL). The reaction solution was stirred at 110°C for 6 hours, the solvent was then evaporated to give a crude residue, which was used for the following reaction without further purification. The residue was redissolved in CH_2Cl_2 (100 mL), and then, compound **3** (1.60 g, 5.0 mmol) and Et_3N (0.61 g, 6.0 mmol) were added. After stirring the mixture at room temperature for 5 hours, CH_2Cl_2 was evaporated, with the residues being taken up in EtOAc (50 mL). The EtOAc solution was washed with saturated aqueous citric acid (3×20 mL), saturated aqueous

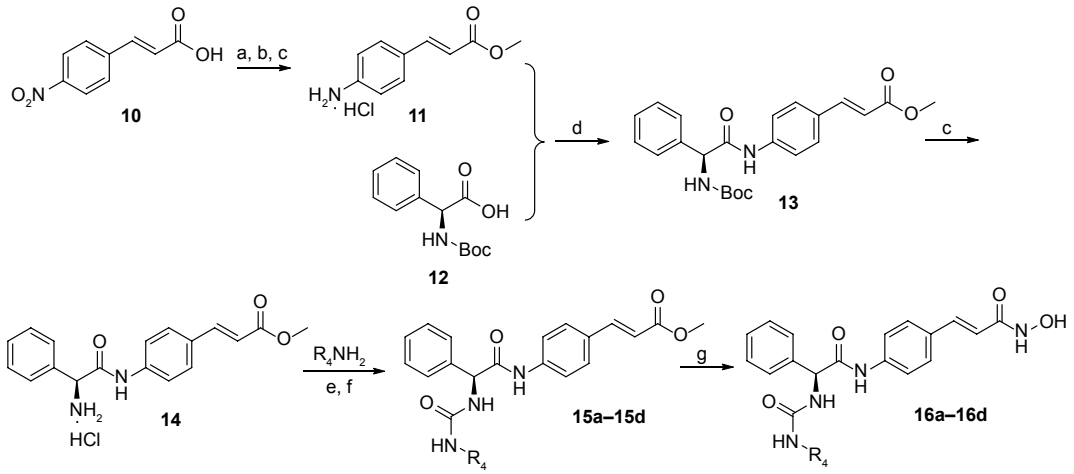

Figure 4 Reagents and conditions: (a) CH_3COCl, MeOH; (b) $SnCl_2$, EtOH; (c) HCl, anhydrous EtOAc; (d) TBTU, Et_3N, DCM; (e) BTC, dioxane, reflux; (f) Et_3N, DCM; (g) NH_2OK, MeOH.
Abbreviations: TBTU, 2-(1*H*-benzotriazole-1-yl)-1,1,3,3-tetramethyluronium tetrafluoroborate; DCM, dichloromethane; BTC, bis(trichloromethyl) carbonate.

$NaHCO_3$ (3×20 mL), and brine (3×20 mL); dried over $MgSO_4$; and concentrated under vacuum. The desired compound **4a** was obtained as a white powder by crystallization from EtOAc (1.08 g, 50%). ^{1}H NMR (300 MHz, DMSO-d_6) δ 10.76 (s, 1H), 8.78 (s, 1H), 7.92 (d, J =9.0 Hz, 2H), 7.73 (d, J =9.0 Hz, 2H), 7.30–7.52 (m, 5H), 7.09–7.15 (m, 3H), 6.82 (dd, J =8.1 Hz, 0.9 Hz, 1H), 6.49 (dd, J=7.8 Hz, 1.8 Hz, 1H), 5.56 (d, J=7.5 Hz, 1H), 3.81 (s, 3H), 3.68 (s, 3H). ESI–MS m/z: 434.2 $[M + H]^+$.

Methyl (*S*)-4-(2-(3-(3-chlorophenyl) ureido)-2-phenylacetamido)benzoate (4b)

Using the similar synthetic method as for **4a**, reaction between compound **3** and 3-chloroaniline gave **4b**, a white powder (44% yield). ESI–MS m/z: 438.1 $[M + H]^+$.

Methyl (*S*)-4-(2-(3-(2-chlorophenyl) ureido)-2-phenylacetamido)benzoate (4c)

Using a similar synthetic method as for **4a**, reaction between compound **3** and 2-chloroaniline gave **4c**, a white powder (31% yield). ESI–MS m/z: 439.2 $[M + H]^+$.

Methyl (*S*)-4-(2-(3-(2-fluorophenyl) ureido)-2-phenylacetamido)benzoate (4d)

Using a similar synthetic method as for **4a**, reaction between compound **3** and 2-fluoroaniline gave **4d**, a white powder (36% yield). ESI–MS m/z: 422.2 $[M + H]^+$.

Methyl (*S*)-4-(2-(3-(2-bromophenyl) ureido)-2-phenylacetamido)benzoate (4e)

Using a similar synthetic method as for **4a**, reaction between compound **3** and 2-bromoaniline gave **4e**, a white powder (43% yield). ESI–MS m/z: 482.0 $[M + H]^+$.

Methyl (*S*)-4-(2-phenyl-2-(3-(*o*-tolyl) ureido)acetamido)benzoate (4f)

Using a similar synthetic method as for **4a**, reaction between compound **3** and *m*-toluidine gave **4f**, a white powder (45% yield). ESI–MS m/z: 418.2 $[M + H]^+$.

Methyl (*S*)-4-(2-phenyl-2-(3-(*p*-tolyl) ureido)acetamido)benzoate (4g)

Using a similar synthetic method as for **4a**, reaction between compound **3** and *p*-toluidine gave **4g**, a white powder (30% yield). ESI–MS m/z: 418.5 $[M + H]^+$.

Methyl (*S*)-4-(2-(3-(2,4-dichlorophenyl) ureido)-2-phenylacetamido)benzoate (4h)

Using a similar synthetic method as for **4a**, reaction between compound **3** and 2,4-dichloroaniline gave **4h**, a white powder (46% yield). ESI–MS m/z: 472.1 $[M + H]^+$.

Methyl (*S*)-4-(2-(3-(3,5-dimethylphenyl) ureido)-2-phenylacetamido)benzoate (4i)

Using a similar synthetic method as for **4a**, reaction between compound **3** and 3,5-dimethylaniline gave **4i**, a white powder (39% yield). ESI–MS m/z: 432.2 $[M + H]^+$.

Methyl (*S*)-4-(2-(3-(2,6-diethylphenyl) ureido)-2-phenylacetamido)benzoate (4j)

Using a similar synthetic method as for **4a**, reaction between compound **3** and 2,6-diethylaniline gave **4j**, a white powder (35% yield). ESI–MS m/z: 460.2 $[M + H]^+$.

Methyl (*S*)-4-(2-(3-(naphthalen-1-yl) ureido)-2-phenylacetamido)benzoate (4k)

Using a similar synthetic method as for **4a**, reaction between compound **3** and naphthalen-1-amine gave **4k**, a white powder (57% yield). ESI–MS m/z: 454.3 $[M + H]^+$.

(*S*)-*N*-Hydroxy-4-(2-(3-(3-methoxyphenyl) ureido)-2-phenylacetamido)benzamide (7a)

To a solution of compound **4a** (0.87 g, 2.0 mmol) in 10 mL of anhydrous methanol, a solution of NH_2OK (0.14 g, 6 mmol) in 3.5 mL of anhydrous methanol was added. The mixture was stirred for 1 hour and the solvent was evaporated under vacuum. The residues were acidified with 2 N HCl until pH 3–4, then extracted with EtOAc (3×10 mL). The organic layers were combined, washed with brine (3×10 mL), dried over $MgSO_4$, and evaporated, with the residues being recrystallized with EtOH/EtOAc to give compound **7a**, a white powder (0.57 g, 66% yield). Mp: 240°C–243°C. ^{1}H NMR (600 MHz, DMSO-d_6) δ 11.07 (s, 1H), 10.66 (s, 1H), 8.80 (s, 1H), 7.71 (d, J =8.4 Hz, 2H), 7.64 (d, J =8.4 Hz, 2H), 7.50 (d, J =7.2 Hz, 2H), 7.40 (t, J =7.8 Hz, 2H), 7.31–7.34 (m, 1H), 7.10–7.15 (m, 3H), 6.81–6.83 (m, 1H), 6.48 (dd, J=7.8 Hz, 2.4 Hz, 1H), 5.55 (d, J=7.8 Hz, 1H), 3.70 (s, 3H). HRMS (atmospheric pressure electrospray ionization [AP–ESI]) m/z: calcd for $C_{23}H_{23}N_4O_5$ $[M + H]^+$, 435.1668; found, 435.1653.

(*S*)-4-(2-(3-(3-Chlorophenyl)ureido)-2-phenylacetamido)-*N*-hydroxybenzamide (7b)

Using a similar synthetic method as for **7a**, compound **4b** gave **7b**, a white powder (70% yield). Mp: 226°C–228°C. ^{1}H NMR (600 MHz, DMSO-d_6) δ 11.11 (s, 1H), 10.65 (s, 1H), 8.95 (s, 1H), 8.28 (s, 1H), 8.15 (d, J=7.8 Hz, 1H), 8.05 (dd, J=7.8 Hz, 1.2 Hz, 1H), 7.71 (d, J =8.4 Hz, 2H), 7.65 (d, J =8.4 Hz, 2H), 7.56 (d, J =7.8 Hz, 1H), 7.53 (d, J =7.2 Hz, 2H), 7.41 (t, J =7.8 Hz, 2H), 7.34 (t, J =7.2 Hz, 1H), 7.25–7.28

(m, 1H), 6.89–6.92 (m, 1H), 5.57 (d, J=7.8 Hz, 1H). HRMS (AP–ESI) m/z: calcd for $C_{22}H_{20}ClN_4O_4$ $[M + H]^+$, 439.1173; found, 439.1170.

(*S*)-4-(2-(3-(2-Chlorophenyl)ureido)-2-phenylacetamido)-*N*-hydroxybenzamide (7c)

Using a similar synthetic method as for **7a**, compound **4c** gave **7c**, a white powder (50% yield). Mp: 228°C–231°C. ^{1}H NMR (600 MHz, DMSO-d_6) δ 11.12 (s, 1H), 10.66 (s, 1H), 8.95 (s, 1H), 8.45 (d, J =4.2 Hz, 1H), 8.14 (dd, J=8.4 Hz, 1.8 Hz, 1H), 8.09 (dd, J=7.8 Hz, 3.0 Hz, 1H), 7.92 (d, J=9.0 Hz, 1H), 7.74 (d, J=9.0 Hz, 1H), 7.71 (d, J=8.4 Hz, 1H), 7.65 (d, J =8.4 Hz, 1H), 7.52–7.53 (m, 2H), 7.40–7.43 (m, 3H), 7.33–7.36 (m, 1H), 7.22 (td, J=7.8 Hz, 1.2 Hz, 1H), 6.96 (td, J =7.8 Hz, 1.2 Hz, 1H), 5.57 (d, J =7.2 Hz). HRMS (AP–ESI) m/z: calcd for $C_{22}H_{20}ClN_4O_4$ $[M + H]^+$, 439.1173; found, 439.1182.

(*S*)-4-(2-(3-(2-Fluorophenyl)ureido)-2-phenylacetamido)-*N*-hydroxybenzamide (7d)

Using a similar synthetic method as for **7a**, compound **4d** gave **7d**, a white powder (57% yield). Mp: 238°C–240°C. ^{1}H NMR (300 MHz, DMSO-d_6) δ 10.61 (s, 1H), 8.77 (s, 1H), 8.11 (td, J =8.4 Hz, 1.5 Hz, 1H), 7.83–7.85 (m, 1H), 7.68 (d, J =8.7 Hz, 2H), 7.58 (d, J =8.7 Hz, 2H), 7.29–7.53 (m, 5H), 6.89–7.23 (m, 3H), 5.57 (d, J =8.1 Hz, 1H). HRMS (AP-ESI) m/z: calcd for $C_{22}H_{20}FN_4O_4$ $[M + H]^+$, 423.1469; found, 423.1466.

(*S*)-4-(2-(3-(2-Bromophenyl)ureido)-2-phenylacetamido)-*N*-hydroxybenzamide (7e)

Using a similar synthetic method as for **7a**, compound **4e** gave **7e**, a white powder (54% yield). Mp: 250°C–252°C. ^{1}H NMR (600 MHz, DMSO-d_6) δ 11.11 (s, 1H), 10.66 (s, 1H), 9.90 (s, 1H), 8.92 (s, 1H), 7.64–7.72 (m, 5H), 7.50 (d, J=7.8 Hz, 2H), 7.40 (t, J=7.8 Hz, 2H), 7.13–7.36 (m, 4H), 6.96 (dd, J =7.8 Hz, 1.2 Hz, 1H), 5.55 (d, J =7.8 Hz, 1H). HRMS (AP–ESI) m/z: calcd for $C_{22}H_{20}BrN_4O_4$ $[M + H]^+$, 483.0668; found, 483.0624.

(*S*)-*N*-Hydroxy-4-(2-phenyl-2-(3-(*o*-tolyl)ureido)acetamido)benzamide (7f)

Using a similar synthetic method as for **7a**, compound **4f** gave **7f**, a white powder (56% yield). Mp: 232°C–233°C. ^{1}H NMR (300 MHz, DMSO-d_6) δ 11.11 (s, 1H), 10.66 (s, 1H), 8.93 (s, 1H), 8.03 (s, 1H), 7.83–7.90 (m, 1H), 7.63–7.73 (m, 5H), 7.30–7.53 (m, 5H), 6.84–7.13 (m, 3H), 5.58 (d, J =7.8 Hz, 1H), 2.18 (s, 3H). HRMS (AP–ESI) m/z: calcd for $C_{23}H_{23}N_4O_4$ $[M + H]^+$, 419.1719; found, 419.1725.

(*S*)-*N*-Hydroxy-4-(2-phenyl-2-(3-(*p*-tolyl)ureido)acetamido)benzamide (7g)

Using a similar synthetic method as for **7a**, compound **4g** gave **7g**, a white powder (50% yield). Mp: 208°C–211°C. ^{1}H NMR (600 MHz, DMSO-d_6) δ 11.11 (s, 1H), 10.65 (s, 1H), 8.95 (s, 1H), 8.66 (s, 1H), 7.71 (d, J =9.0 Hz, 2H), 7.64 (d, J =9.0 Hz, 2H), 7.49 (d, J =7.8 Hz, 2H), 7.40 (t, J=7.8 Hz, 2H), 7.32 (t, J=7.8 Hz, 1H), 7.25 (d, J=8.4 Hz, 2H), 7.08 (d, J=8.4 Hz, 1H), 7.03 (d, J=7.8 Hz, 2H), 5.56 (d, J=7.8 Hz, 1H), 2.21 (s, 3H). HRMS (AP–ESI) m/z: calcd for $C_{23}H_{23}N_4O_4$ $[M + H]^+$, 419.1719; found, 419.1723.

(*S*)-4-(2-(3-(2,4-Dichlorophenyl)ureido)-2-phenylacetamido)-*N*-hydroxybenzamide (7h)

Using a similar synthetic method as for **7a**, compound **4h** gave **7h**, a white powder (67% yield). Mp: 213°C–215°C. ^{1}H NMR (300 MHz, DMSO-d_6) δ 11.09 (s, 1H), 10.65 (s, 1H), 8.93 (s, 1H), 8.54 (s, 1H), 8.12–8.19 (m, 2H), 7.29–7.73 (m, 11H), 5.57 (d, J=7.5 Hz, 1H). HRMS (AP–ESI) m/z: calcd for $C_{22}H_{19}Cl_2N_4O_4$ $[M + H]^+$, 473.0783; found, 473.0784.

(*S*)-4-(2-(3-(3,5-Dimethylphenyl)ureido)-2-phenylacetamido)-*N*-hydroxybenzamide (7i)

Using a similar synthetic method as for **7a**, compound **4i** gave **7i**, a white powder (65% yield). Mp: 276°C–278°C. ^{1}H NMR (300 MHz, DMSO-d_6) δ 10.54 (s, 1H), 8.91 (s, 1H), 7.86 (s, 1H), 7.21–7.68 (m, 10H), 7.02 (d, J =8.7 Hz, 2H), 6.47–6.53 (m, 1H), 5.50–5.54 (m, 1H), 2.19 (s, 6H). HRMS (AP–ESI) m/z: calcd for $C_{24}H_{25}N_4O_4$ $[M + H]^+$, 433.1876; found, 433.1878.

(*S*)-4-(2-(3-(2,6-Diethylphenyl)ureido)-2-phenylacetamido)-*N*-hydroxybenzamide (7j)

Using a similar synthetic method as for **7a**, compound **4j** gave **7j**, a white powder (% yield). Mp: 230°C–232°C. ^{1}H NMR (600 MHz, DMSO-d_6) δ 11.12 (s, 1H), 10.64 (s, 1H), 8.95 (s, 1H), 7.78 (s, 1H), 7.71 (d, J =8.4 Hz, 2H), 7.65 (d, J=8.4 Hz, 2H), 7.48–7.54 (m, 2H), 7.40 (t, J=7.2 Hz, 2H), 3.14 (t, J=7.2 Hz, 1H), 7.05–7.11 (m, 4H), 5.57 (d, J=8.4 Hz, 1H), 2.52 (q, J =9.6 Hz, 4H), 1.06 (t, J =9.6 Hz, 6H). HRMS (AP–ESI) m/z: calcd for $C_{26}H_{29}N_4O_4$ $[M + H]^+$, 461.2189; found, 461.2194.

(*S*)-*N*-Hydroxy-4-(2-(3-(naphthalen-1-yl) ureido)-2-phenylacetamido)benzamide (7k)

Using a similar synthetic method as for **7a**, compound **4k** gave **7k**, a white powder (50% yield). Mp: 218°C–221°C. ^{1}H NMR (600 MHz, DMSO-d_6) δ 11.14 (s, 1H), 10.78 (s, 1H), 8.99 (s, 1H), 8.96 (s, 1H), 8.20 (d, J =9.0 Hz, 1H), 8.04 (d, J =7.8 Hz, 1H), 7.89 (d, J =7.8 Hz, 1H), 7.82 (d, J =7.2 Hz, 1H), 7.68–7.73 (m, 4H), 7.49–7.59 (m, 5H), 7.32–7.43 (m, 4H), 5.66 (d, J =7.8 Hz, 1H). HRMS (AP–ESI) *m*/*z*: calcd for $C_{26}H_{23}N_4O_4$ $[M + H]^+$, 455.1719; found, 455.1730.

Methyl (*S*)-4-(2-phenyl-2-(quinoline-6-carboxamido)acetamido)benzoate (5a)

At room temperature, to a solution of quinoline-6-carboxylic acid (0.17 g, 1.0 mmol) in anhydrous CH_2Cl_2 (20 mL), Et_3N (0.11 g, 1.1 mmol) followed by 2-(1*H*-benzotriazole-1-yl)-1,1,3,3-tetramethyluronium tetrafluoroborate (0.35 g, 1.1 mmol) was added. After 15 minutes, compound **3** (0.32 g, 1.0 mmol) and Et_3N (0.11 g, 1.1 mmol) were added. Stirring was continued until compound **3** disappeared by TLC, then CH_2Cl_2 was evaporated with the residue being taken up in EtOAc (50 mL). The EtOAc solution was washed with saturated aqueous citric acid (3×20 mL), saturated aqueous $NaHCO_3$ (3×20 mL), and brine (3×20 mL); dried over $MgSO_4$; and evaporated with the residue being purified by flash column chromatography (petroleum/EtOAc 2:1) to give compound **5a**, a white powder (0.23 g, 52% yield). ^{1}H NMR (300 MHz, DMSO-d_6) δ 10.75 (s, 1H), 9.30 (d, J =7.2 Hz, 1H), 9.00 (dd, J =4.2, 1.8 Hz, 1H), 8.66 (d, J =1.8 Hz, 1H), 8.49 (d, J =7.2 Hz, 1H), 8.23 (dd, J =9.0, 1.8 Hz, 1H), 8.08 (d, J =9.0 Hz, 1H), 7.93 (d, J =8.7 Hz, 2H), 7.77 (d, J =8.7 Hz, 2H), 7.60–7.64 (m, 3H), 7.34–7.46 (m, 3H), 5.90 (d, J =7.2 Hz, 1H), 3.82 (s, 3H). ESI–MS *m*/*z*: 440.1 $[M + H]^+$.

Methyl (*S*)-4-(2-phenyl-2-(quinoxaline-6-carboxamido)acetamido)benzoate (5b)

Using a similar synthetic method as for **5a**, compound **3** and quinoxaline-6-carboxylic acid gave **5b**, a white powder (41% yield). ESI–MS *m*/*z*: 441.1 $[M + H]^+$.

Methyl (*S*)-4-(2-(1*H*-indole-6-carboxamido)-2-phenylacetamido)benzoate (5c)

Using a similar synthetic method as for **5a**, compound **3** and 1*H*-indole-6-carboxylic acid gave **5c**, a white powder (37% yield). ESI–MS *m*/*z*: 428.7 $[M + H]^+$.

Methyl (*S*)-4-(2-(1*H*-indole-2-carboxamido)-2-phenylacetamido)benzoate (5d)

Using a similar synthetic method as for **5a**, compound **3** and 1*H*-indole-2-carboxylic acid gave **5d**, a white powder (53% yield). ESI–MS *m*/*z*: 428.7 $[M + H]^+$.

Methyl (*S*)-4-(2-phenyl-2-(pyrazine-2-carboxamido)acetamido)benzoate (5e)

Using a similar synthetic method as for **5a**, compound **3** and pyrazine-2-carboxylic acid gave **5e**, a white powder (76% yield). ESI–MS *m*/*z*: 391.0 $[M + H]^+$.

(*S*)-*N*-(2-((4-(Hydroxycarbamoyl)phenyl) amino)-2-oxo-1-phenylethyl)quinoline-6-carboxamide (8a)

Using a similar synthetic method as for **7a**, compound **5a** gave **8a**, a white powder (64% yield). Mp: 222°C–225°C. ^{1}H NMR (400 MHz, DMSO-d_6) δ 11.13 (s, 1H), 10.67–10.80 (m, 2H), 9.39 (s, 1H), 9.10 (s, 1H), 8.67–8.74 (m, 2H), 8.15–8.33 (m, 2H), 7.37–7.90 (m, 10H), 5.93 (s, 1H). HRMS (AP–ESI) *m*/*z*: calcd for $C_{25}H_{21}N_4O_4$ $[M + H]^+$, 441.1563; found, 441.1569.

(*S*)-*N*-(2-((4-(Hydroxycarbamoyl)phenyl) amino)-2-oxo-1-phenylethyl)quinoxaline-6-carboxamide (8b)

Using a similar synthetic method as for **7a**, compound **5b** gave **8b**, a white powder (57% yield). Mp: 180°C–182°C. ^{1}H NMR (400 MHz, DMSO-d_6) δ 11.12 (s, 1H), 10.65 (s, 1H), 9.51–9.57 (m, 1H), 9.04–9.05 (m, 2H), 8.72–8.75 (m, 1H), 8.17–8.32 (m, 2H), 7.37–7.74 (m, 10H), 5.91 (d, J =7.2 Hz, 1H). HRMS (AP–ESI) *m*/*z*: calcd for $C_{24}H_{20}N_5O_4$ $[M + H]^+$, 442.1515; found, 442.1511.

(*S*)-*N*-(2-((4-(Hydroxycarbamoyl)phenyl) amino)-2-oxo-1-phenylethyl)-1*H*-indole-6-carboxamide (8c)

Using a similar synthetic method as for **7a**, compound **5c** gave **8c**, a white powder (47% yield). Mp: 146°C–148°C. ^{1}H NMR (400 MHz, DMSO-d_6) δ 11.34 (s, 1H), 11.17 (s, 1H), 10.56 (s, 1H), 8.78 (d, J =7.6 Hz, 1H), 8.27 (s, 1H), 7.40–7.71 (m, 13H), 6.54 (s, 1H), 5.88 (d, J =7.6 Hz, 1H). HRMS (AP–ESI) *m*/*z*: calcd for $C_{24}H_{21}N_4O_4$ $[M + H]^+$, 429.1563; found, 429.1573.

(*S*)-*N*-(2-((4-(Hydroxycarbamoyl)phenyl) amino)-2-oxo-1-phenylethyl)-1*H*-indole-2-carboxamide (8d)

Using a similar synthetic method as for **7a**, compound **5d** gave **8d**, a white powder (59% yield). Mp: 231°C–233°C. ^{1}H NMR (400 MHz, DMSO-d_6) δ 11.74 (s, 1H), 11.18

(s, 1H), 10.93 (s, 1H), 9.14 (d, J =7.6 Hz, 1H), 8.97 (s, 1H), 7.61–7.74 (m, 7H), 7.05–7.45 (m, 7H), 5.96 (d, J =7.6 Hz, 1H). HRMS (AP–ESI) m/z: calcd for $C_{24}H_{21}N_4O_4$ $[M + H]^+$, 429.1563; found, 429.1566.

(*S*)-*N*-(2-((4-(Hydroxycarbamoyl)phenyl) amino)-2-oxo-1-phenylethyl)pyrazine-2-carboxamide (8e)

Using a similar synthetic method as for **7a**, compound **5e** gave **8e**, a white powder (63% yield). Mp: 150°C–152°C. ^{1}H NMR (400 MHz, DMSO-d_6) δ 11.15 (s, 1H), 10.77–10.81 (m, 2H), 9.21 (d, J =1.2 Hz, 1H), 9.08 (d, J =7.6 Hz, 1H), 8.94 (d, J =2.4 Hz, 1H), 8.81 (dd, J =2.4, 1.6 Hz, 1H), 7.73 (t, J =8.8 Hz, 2H), 7.67 (d, J =8.8 Hz, 2H), 7.35–7.59 (m, 5H), 5.89 (d, J =7.6 Hz, 1H). HRMS (AP–ESI) m/z: calcd for $C_{20}H_{18}N_5O_4$ $[M + H]^+$, 392.1359; found, 392.1375.

Methyl (*S*)-4-(2-((2-methoxybenzyl) amino)-2-phenylacetamido)benzoate (6a)

To a solution of compound **3** (1.60 g, 5.0 mmol), Et_3N (0.50 g, 5.0 mmol), and 2-methoxybenzaldehyde (0.81 g, 24.0 mmol) in EtOH (50 mL), acetic acid and sodium cyanoborohydride (1.98 g, 24.0 mmol) were added dropwise. The mixture was stirred at room temperature for 12 hours, and the solvent was evaporated under vacuum. The residue was purified by flash column chromatography (petroleum ether/EtOAc 3:1) to give compound **6a** (1.13 g, 56% yield), a white powder. ^{1}H NMR (300 MHz, DMSO-d_6) δ 10.40 (s, 1H), 7.90 (d, J =6.9 Hz, 2H), 7.75 (d, J =6.9 Hz, 2H), 7.20–7.50 (m, 7H), 6.90–6.96 (m, 2H), 4.40 (s, 1H), 3.81 (s, 3H), 3.73 (s, 3H), 3.68 (s, 2H), 3.06 (s, 1H). ESI–MS m/z: 405.5 $[M + H]^+$.

Methyl (*S*)-4-(2-((2-chlorobenzyl)amino)-2-phenylacetamido)benzoate (6b)

Using a similar synthetic method as for **6a**, reaction between compound **3** and 2-chlorobenzaldehyde gave **6b**, a white powder (39% yield). ESI–MS m/z: 409.5 $[M + H]^+$.

Methyl (*S*)-4-(2-((2-bromobenzyl)amino)-2-phenylacetamido)benzoate (6c)

Using a similar synthetic method as for **6a**, reaction between compound **3** and 2-bromobenzaldehyde gave **6c**, a white powder (40% yield). ESI–MS m/z: 453.0 $[M + H]^+$.

Methyl (*S*)-4-(2-((3-methoxybenzyl) amino)-2-phenylacetamido)benzoate (6d)

Using a similar synthetic method as for **6a**, reaction between compound **3** and 3-methoxybenzaldehyde gave **6d**, a white powder (57% yield). ESI–MS m/z: 405.5 $[M + H]^+$.

Methyl (*S*)-4-(2-((4-chlorobenzyl)amino)-2-phenylacetamido)benzoate (6e)

Using a similar synthetic method as for **6a**, reaction between compound **3** and 4-chlorobenzaldehyde gave **6e** as a light yellow oil (48% yield). ESI–MS m/z: 409.5 $[M + H]^+$.

Methyl (*S*)-4-(2-((4-hydroxybenzyl)amino)-2-phenylacetamido)benzoate (6f)

Using a similar synthetic method as for **6a**, reaction between compound **3** and 4-hydroxybenzaldehyde gave **6f** as a light yellow oil (64% yield). ESI–MS m/z: 391.2 $[M + H]^+$.

Methyl (*S*)-4-(2-((4-hydroxy-3-methoxybenzyl)amino)-2-phenylacetamido)benzoate (6g)

Using a similar synthetic method as for **6a**, reaction between compound **3** and 4-hydroxy-3-methoxybenzaldehyde gave **6g** as a light yellow oil (65% yield). ESI–MS m/z: 421.2 $[M + H]^+$.

(*S*)-*N*-Hydroxy-4-(2-((2-methoxybenzyl) amino)-2-phenylacetamido)benzamide (9a)

To a solution of compound **6a** (0.81 g, 2.0 mmol) in 10 mL of anhydrous methanol, a solution of NH_2OK (0.14 g, 6 mmol) in 3.5 mL of anhydrous methanol was added. The mixture was stirred for 1 hour and the solvent was evaporated under vacuum. The pH value of residues was adjusted with 2 N HCl and 1 N NaOH until the maximum precipitates were generated, which were then extracted with EtOAc (3×20 mL). The organic layers were combined, washed with brine (3×10 mL), dried over $MgSO_4$, and concentrated, with the residues being stirred with EtOAc saturated by dry HCl (10 mL) for 20 minutes. The precipitates were filtered, with the filter being washed with EtOAc to get compound **9a** (0.57 g, 64% yield), a white powder. Mp: 160°C–162°C. ^{1}H NMR (400 MHz, DMSO-d_6) δ 11.40 (s, 1H), 9.87–9.96 (m, 2H), 7.47–7.74 (m, 6H), 7.30–7.46 (m, 5H), 6.97–7.07 (m, 2H), 5.17 (t, J =6.0 Hz, 1H), 3.99–4.14 (m, 2H), 3.74 (s, 3H). HRMS (AP–ESI) m/z: calcd for $C_{23}H_{24}N_3O_4$ $[M + H]^+$, 406.1767; found, 406.1742.

(*S*)-4-(2-((2-Chlorobenzyl)amino)-2-phenylacetamido)-*N*-hydroxybenzamide (9b)

Using a similar synthetic method as for **7a**, compound **6b** gave **9b**, a white powder (70% yield). Mp: 200°C–202°C. ^{1}H NMR (400 MHz, DMSO-d_6) δ 11.39 (s, 1H), 10.22–10.36 (m, 2H), 7.65–7.81 (m, 7H), 7.42–7.54 (m, 6H), 5.32 (s, 1H),

4.23 (s, 2H). HRMS (AP–ESI) *m/z*: calcd for $C_{22}H_{21}ClN_3O_3$ $[M + H]^+$, 410.1271; found, 410.1272.

(*S*)-4-(2-((2-Bromobenzyl)amino)-2-phenylacetamido)-*N*-hydroxybenzamide (9c)

Using a similar synthetic method as for **7a**, compound **6c** gave **9c**, a white powder (54% yield). Mp: 220°C–222°C. ^{1}H NMR (400 MHz, DMSO-d_6) δ 11.39 (s, 1H), 11.25 (s, 1H), 10.22–10.39 (m, 2H), 8.93 (d, J =4.0 Hz, 1H), 7.66–7.72 (m, 8H), 7.47–7.50 (m, 5H), 5.32 (s, 1H), 4.24 (s, 2H). HRMS (AP–ESI) *m/z*: calcd for $C_{22}H_{21}BrN_3O_3$ $[M + H]^+$, 454.0766; found, 454.0756.

(*S*)-*N*-Hydroxy-4-(2-((3-methoxybenzyl)amino)-2-phenylacetamido)benzamide (9d)

Using a similar synthetic method as for **7a**, compound **6d** gave **9d**, a white powder (65% yield). Mp: 184°C–189°C. ^{1}H NMR (400 MHz, DMSO-d_6) δ 11.35 (s, 1H), 10.16–10.33 (m, 2H), 7.50–7.74 (m, 6H), 7.47–7.48 (m, 3H), 7.31–7.32 (m, 1H), 6.96–7.15 (m, 3H), 5.20 (t, J =6.0 Hz, 1H), 4.00–4.10 (m, 2H), 3.76 (s, 3H). HRMS (AP–ESI) *m/z*: calcd for $C_{23}H_{24}N_3O_4$ $[M + H]^+$, 406.1767; found, 406.1743.

(*S*)-4-(2-((4-Chlorobenzyl)amino)-2-phenylacetamido)-*N*-hydroxybenzamide (9e)

Using a similar synthetic method as for **7a**, compound **6e** gave **9e**, a white powder (58% yield). Mp: 193°C–195°C. ^{1}H NMR (400 MHz, DMSO-d_6) δ 11.47 (s, 1H), 10.22–10.37 (m, 2H), 7.66–7.75 (m, 6H), 7.46–7.55 (m, 7H), 5.27 (s, 1H), 4.02–4.12 (m, 2H). HRMS (AP–ESI) *m/z*: calcd for $C_{22}H_{21}ClN_3O_3$ $[M + H]^+$, 410.1271; found, 410.1283.

(*S*)-*N*-Hydroxy-4-(2-((4-hydroxybenzyl)amino)-2-phenylacetamido)benzamide (9f)

Using a similar synthetic method as for **7a**, compound **6f** gave **9f**, a white powder (46% yield). Mp: 240°C–242°C. ^{1}H NMR (400 MHz, DMSO-d_6) δ 11.35 (s, 1H), 10.30 (s, 1H), 10.00–10.08 (m, 2H), 7.30–7.91 (m, 6H), 7.44–7.49 (m, 3H), 7.27 (d, J =8.4 Hz, 2H), 6.81 (d, J =10.0 Hz, 2H), 5.16 (t, J =6.0 Hz, 1H), 3.89–3.97 (m, 2H). HRMS (AP–ESI) *m/z*: calcd for $C_{22}H_{22}N_3O_4$ $[M + H]^+$, 392.1610; found, 392.1607.

(*S*)-*N*-Hydroxy-4-(2-((4-hydroxy-3-methoxybenzyl)amino)-2-phenylacetamido)benzamide (9g)

Using a similar synthetic method as for **7a**, compound **6g** gave **9g**, a white powder (42% yield). Mp: 168°C–170°C. ^{1}H NMR (400 MHz, DMSO-d_6) δ 11.22 (s, 1H), 9.99–10.09 (m, 2H), 7.63–7.74 (m, 6H), 7.45–7.52 (m, 3H), 7.10 (s, 1H), 6.80 (s, 2H), 5.08 (t, J =6.0 Hz, 1H), 3.90–3.99 (m, 2H), 3.76 (s, 3H). HRMS (AP–ESI) *m/z*: calcd for $C_{23}H_{24}N_3O_5$ $[M + H]^+$, 422.1716; found, 422.1718.

Methyl (*E*)-3-(4-aminophenyl)acrylate hydrochloride (11)

Compound **10** (9.66 g, 50.0 mmol) was dissolved in 200 mL of methanol; then acetyl chloride (11.78 g, 150.0 mmol) was added dropwise at 0°C; the mixed solution was refluxed at 70°C for 6 hours. The solvent was evaporated under vacuum to get crude methyl (*E*)-3-(4-nitrophenyl)acrylate, which was used for the following reaction without further purification. To a solution of methyl (*E*)-3-(4-nitrophenyl)acrylate (0.21 g, 1.0 mmol) in 30 mL of ethanol, stannous chloride dehydrate (1.13 g, 5.0 mmol) was added, and the mixture was refluxed at 75°C for 4 hours. The solvent was evaporated under vacuum followed by addition of 30 mL of distilled water, then saturated $NaHCO_3$ was added until no more gas was generated. The mixture was extracted with EtOAc (3×20 mL). The organic layers were combined, washed with brine (3×10 mL), dried over $MgSO_4$, and concentrated, with the residues being stirred with EtOAc saturated by dry HCl (10 mL) for 20 minutes. The precipitates were filtered, with the filter being washed with EtOAc to get compound **11** (0.19 g, 89% yield), a white powder. ESI–MS *m/z*: 178.0 $[M + H]^+$.

(*S*)-2-((*tert*-Butoxycarbonyl)amino)-2-phenylacetic acid (12)

Compound **12** was synthesized according to the methods described in our previous study.[5]

Methyl (*S*, *E*)-3-(4-(2-((*tert*-butoxycarbonyl)amino)-2-phenylacetamido)phenyl)acrylate (13)

Using a similar synthetic method as for **5a**, reaction between compound **12** and **11** gave **13**, a white powder (76% yield). ESI–MS *m/z*: 411.2 $[M + H]^+$.

Methyl (*S*, *E*)-3-(4-(2-amino-2-phenylacetamido)phenyl)acrylate (14)

To a solution of compound **13** (0.41 g, 1.0 mmol) in dry EtOAc (15 mL), a solution of EtOAc (15 mL) saturated by dry HCl was added. The resulting solution was continuously stirred (for 5 hours) at room temperature until the precipitates appeared. The suspension was filtered, with the filter being washed with ether to give compound **14** (0.30 g, 86% yield), a white powder. ESI–MS *m/z*: 311.2 $[M + H]^+$.

Methyl (*S*, *E*)-3-(4-(2-(3-(2-chlorophenyl) ureido)-2-phenylacetamido)phenyl) acrylate (15a)

Using a similar synthetic method as for **4a**, reaction between compound **14** and 2-chloroaniline gave **15a**, a white powder (46% yield). ^{1}H NMR (400 MHz, DMSO-d_6) δ 10.73 (s, 1H), 8.46 (s, 1H), 8.10–8.14 (m, 2H), 7.66–7.68 (m, 4H), 7.59 (d, J =16.0 Hz, 1H), 6.80–7.55 (m, 8H), 6.53 (d, J =16.0 Hz, 1H), 5.59 (d, J =8.4 Hz, 1H), 3.71 (s, 3H). ESI–MS m/z: 464.1 $[M + H]^+$.

Methyl (*S*, *E*)-3-(4-(2-(3-(2-fluorophenyl) ureido)-2-phenylacetamido)phenyl) acrylate (15b)

Using a similar synthetic method as for **4a**, reaction between compound **14** and 2-fluoroaniline gave **15b**, a white powder (49% yield). ESI–MS m/z: 448.2 $[M + H]^+$.

Methyl (*S*, *E*)-3-(4-(2-(3-(2-bromophenyl) ureido)-2-phenylacetamido)phenyl) acrylate (15c)

Using a similar synthetic method as for **4a**, reaction between compound **14** and 2-bromoaniline gave **15c**, a white powder (51% yield). ESI–MS m/z: 408.0 $[M + H]^+$.

Methyl (*S*, *E*)-3-(4-(2-phenyl-2-(3-(*o*-tolyl) ureido)acetamido)phenyl)acrylate (15d)

Using a similar synthetic method as for **4a**, reaction between compound **14** and *o*-toluidine gave **15d**, a white powder (45% yield). ESI–MS m/z: 444.2 $[M + H]^+$.

(*S*, *E*)-3-(4-(2-(3-(2-Chlorophenyl) ureido)-2-phenylacetamido)phenyl)-*N*-hydroxyacrylamide (16a)

Using a similar synthetic method as for **7a**, compound **15a** gave **16a**, a white powder (66% yield). Mp: 184°C–186°C. ^{1}H NMR (400 MHz, DMSO-d_6) δ 10.78 (s, 1H), 10.73 (s, 1H), 10.10 (s, 1H), 8.19 (s, 1H), 6.95–8.14 (m, 15H), 6.53 (d, J =16.0 Hz, 1H), 5.60 (d, J =5.2 Hz, 1H). HRMS (AP–ESI) m/z: calcd for $C_{24}H_{22}ClN_4O_4$ $[M + H]^+$, 465.1330; found, 465.1334.

(*S*, *E*)-3-(4-(2-(3-(2-Fluorophenyl) ureido)-2-phenylacetamido)phenyl)-*N*-hydroxyacrylamide (16b)

Using a similar synthetic method as for **7a**, compound **15b** gave **16b**, a white powder (60% yield). Mp: 226°C–228°C. ^{1}H NMR (600 MHz, DMSO-d_6) δ 10.72 (s, 1H), 10.65 (s, 1H), 9.01 (s, 1H), 8.71 (s, 1H), 8.10 (td, J =8.4 Hz, 1.8 Hz, 1H), 7.73 (d, J =8.4 Hz, 1H), 7.64 (d, J =7.8 Hz, 2H), 7.50–7.52 (m, 4H), 7.32–7.42 (m, 4H), 7.17–7.20 (m, 1H), 7.07 (t, J =7.2 Hz, 1H), 6.91–6.95 (m, 1H), 6.36 (d, J =16.2 Hz, 1H), 5.58 (d, J =7.8 Hz, 1H). HRMS (AP–ESI) m/z: calcd for $C_{24}H_{22}FN_4O_4$ $[M + H]^+$, 449.1625; found, 449.1620.

(*S*, *E*)-3-(4-(2-(3-(2-Bromophenyl) ureido)-2-phenylacetamido)phenyl)-*N*-hydroxyacrylamide (16c)

Using a similar synthetic method as for **7a**, compound **15c** gave **16c**, a white powder (59% yield). Mp: 185°C–187°C. ^{1}H NMR (600 MHz, DMSO-d_6) δ 10.71 (s, 1H), 10.62 (s, 1H), 9.01 (s, 1H), 8.28 (s, 1H), 8.15 (d, J =7.8 Hz, 1H), 8.04 (dd, J =8.4 Hz, 1.2 Hz, 1H), 7.65 (d, J =8.4 Hz, 2H), 7.56 (dd, J =7.8 Hz, 1.2 Hz, 1H), 7.51–7.53 (m, 4H), 7.25–7.43 (m, 5H), 6.90 (td, J =7.2 Hz, 1.8 Hz, 1H), 6.35 (d, J =16.2 Hz, 1H), 5.57 (d, J =7.2 Hz, 1H). HRMS (AP–ESI) m/z: calcd for $C_{24}H_{22}BrN_4O_4$ $[M + H]^+$, 509.0824; found, 509.0820.

(*S*, *E*)-*N*-Hydroxy-3-(4-(2-phenyl-2-(3-(o-tolyl)ureido)acetamido)phenyl)acrylamide (16d)

Using a similar synthetic method as for **7a**, compound **15d** gave **16d**, a white powder (47% yield). Mp: 194°C–196°C. ^{1}H NMR (600 MHz, DMSO-d_6) δ 10.74 (s, 1H), 10.68 (s, 1H), 9.02 (s, 1H), 8.76 (s, 1H), 8.06–8.08 (m, 1H), 7.85 (d, J =7.2 Hz, 1H), 7.65–7.70 (m, 3H), 7.50–7.54 (m, 3H), 7.31–7.42 (m, 4H), 7.06–7.12 (m, 2H), 6.85–6.87 (m, 1H), 6.37 (d, J =16.2 Hz, 1H), 5.57 (d, J =7.2 Hz, 1H), 2.20 (s, 3H). HRMS (AP–ESI) m/z: calcd for $C_{25}H_{25}N_4O_4$ $[M + H]^+$, 445.1876; found, 445.1866.

Biological materials and methods

In vitro HDAC inhibition fluorescence assay

In vitro HDAC inhibition assays were conducted as previously described.[8,10–12] In brief, 10 μL of enzyme solution (HeLa cell nuclear extract) was mixed with different concentrations of tested compound (50 μL). The mixture was incubated at 37°C for 10 minutes, then substrate Boc-Lys (acetyl)-AMC (40 μL) was added. After incubation at 37°C for 30 minutes, the reaction was stopped by the addition of 100 μL of developer containing trypsin and Trichostatin A (a very potent HDAC inhibitor used here to completely stop the deacetylation reaction). Fluorescence intensity was measured after 20 minutes using a microplate reader at excitation and emission wavelengths of 390 and 460 nm, respectively. The inhibition ratios were calculated from the fluorescence

intensity readings of inhibited wells relative to those of control wells, and the half-maximal inhibitory concentration (IC_{50}) values were determined using a regression analysis of the concentration/inhibition ratio.

In vitro antiproliferative assay

In vitro antiproliferative assays were determined by the MTT (3-[4,5-dimethyl-2-thiazolyl]-2,5-diphenyl-2*H*-tetrazolium bromide) method as previously described.[8,10–12] Briefly, human histiocytic lymphoma U937, human multiple myeloma U266, human acute myelogenous leukemia KG-1, human cervical cancer HeLa, human hepatoma H7402, and human colon carcinoma HCT116 cells were individually maintained in Roswell Park Memorial Institute-1640 (RPMI-1640) medium containing 10% fetal bovine serum at 37°C in 5% CO_2 humidified incubator. Cells were passaged the day before dosing into a 96-well cell plate and allowed to grow for a minimum of 4 hours prior to addition of compounds. After addition of compounds, the plates were incubated for an additional 48 hours, and then 0.5% MTT solution was added to each well. After further incubation for 4 hours, the formazan formed from MTT was extracted by adding 200 μL of DMSO for 15 minutes. Absorbance was then determined using an ELISA reader at 570 nm. The inhibition ratios were calculated from the optical density readings of inhibited wells relative to those of control wells, and the IC_{50} values were calculated using a regression analysis of the concentration/inhibition ratio.

In vivo antitumor assay in U937 xenograft model

In vivo human tumor xenograft models were established as previously described.[8,10–12] In brief, tumor cell line (U937) were cultured in RPMI-1640 medium containing 10% fetal bovine serum and maintained in a 5% CO_2 humidified incubator at 37°C. For in vivo antitumor assays, the aforementioned cells were subcutaneously inoculated in the right flanks of male athymic nude mice (BALB/c-nu, 5–6 weeks old, Beijing HFK Bioscience Co., Ltd., People's Republic of China). Approximately 10 days after injection, tumors were palpable (~100 mm^3) and the mice were randomized into treatment and control groups (six mice per group). The treatment groups were dosed orally with either **9d** (100 mg/kg once a day) or SAHA (100 mg/kg once a day) for 12 days, and the blank control group received an equal volume of phosphate-buffered saline solution. During treatment, subcutaneous tumors were measured using a vernier caliper every 3 days, and body weight was regularly monitored. Tumor volumes (V) were estimated using the equation, $V = ab^2/2$, where a and b denote the longest and shortest diameter, respectively. Relative increment ratio (T/C) was calculated according to the following formula:

$$T/C\ (\%) = \frac{\text{The treatment group } (T) \text{ RTV}}{\text{The blank control group } (C) \text{ RTV}}$$

RTV, namely relative tumor volume = V_t/V_0 (V_t: the tumor volume measured each time during the treatment; V_0: the tumor volume measured at the time of randomization).

After treatment, mice were sacrificed and dissected to weigh the tumor tissues and to examine the internal organ injury by macroscopic analysis. All the obtained data were used to evaluate the antitumor potency and toxicity of compounds. Data were analyzed by Student's two-tailed t-test. A P-level <0.05 was considered statistically significant. All experiments involving laboratory animals were performed with the approval of the Shandong University Laboratory Animal Center ethics committee.

Results and discussion

In vitro HDAC inhibitory activities of all synthesized compounds were evaluated using HeLa cell nuclear extracts as enzyme source.[10–12] Results listed in Table 1 show that all ureido analogs **7a**–**7k** except **7j** exhibited more potent HDAC inhibitory activities than SAHA. Generally, ortho and para substitutions were well tolerated. For example, ortho-substituted **7c**, **7e**, **7f** and para-substituted **7g** were better than their lead compound **D18**, and the most potent analog **7h** was ortho and para disubstituted. Compounds with larger R_1 groups, such as **7j** and **7k** exhibited decreased potency. *N*-Hydroxycinnamamide is a very popular fragment in HDAC inhibitor design, which is contained in the structures of approved drug LBH-589, PXD101, and clinical compound SB-939 (Figure 1). Based on the *N*-hydroxycinnamamide fragment, we previously developed a series of HDAC inhibitors with remarkable in vitro and in vivo antitumor activities.[10] However, introduction of *N*-hydroxycinnamamide fragment was detrimental to our compounds described here. *N*-Hydroxycinnamamide-based compounds **16a**–**16d** exhibited much lesser rates of HDAC inhibition compared with their *N*-hydroxybenzamide analogs **7c**–**7f** (Table 1).

HDAC inhibitory activities of amide series compounds (listed in Table 2) demonstrated that replacing the naphthyl group of **D3** and the phenyl group of **D7** with aromatic heterocycles was detrimental to their HDAC inhibitory activities.

Encouraged by their potent HDAC inhibitory activities, several representative ureido compounds **7a**, **7b**, **7c**,

Table 1 HDAC inhibitory activities of ureido series compounds

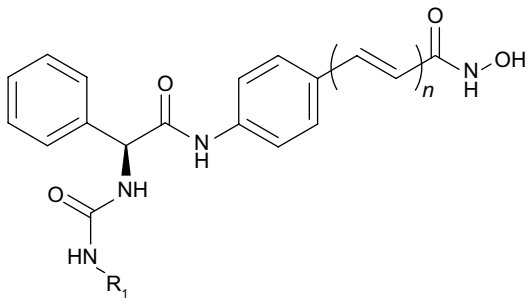

Compound	R_1	*n*	HeLa cell nuclear extract IC_{50} (nM)[a]
SAHA[b]	–	–	145.6
D18[b]	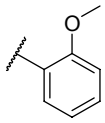	0	7.5
7a	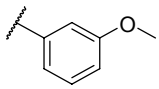	0	13.3
7b	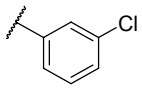	0	12.6
7c	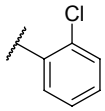	0	2.3
7d	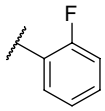	0	76.1
7e	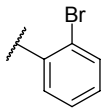	0	4.1
7f	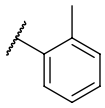	0	6.3
7g	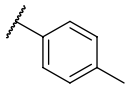	0	2.7
7h	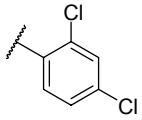	0	1.2
7i	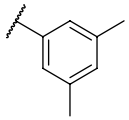	0	15.0
7j	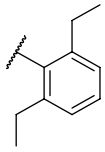	0	178.2
7k	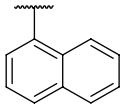	0	124.5
16a	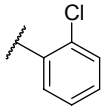	1	128.0
16b	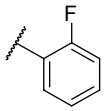	1	215.2
16c	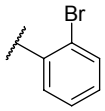	1	91.7
16d	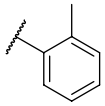	1	811.0

Notes: [a]Values are the mean of three experiments. The standard derivations are <20% of the mean. [b]Data from Zhang et al.[8]

Abbreviations: SAHA, suberoylanilide hydroxamic acid; IC_{50}, half-maximal inhibitory concentration; HDAC, histone deacetylase.

7e, **7g**, **7h**, and **7i** were selected to test their effects on the viability of U937 cell line. Considering the fact that amide compounds **8a**–**8d** might have better water solubility than their parent compound **D3**, their antiproliferative potency were also evaluated even though their HDAC inhibitory activities were not satisfying. The results listed in Table 3 showed that all the tested ureido compounds, including **7c**, **7e**, **7g**, and **7h**, which possessed superior HDAC inhibition to their parent compound **D18**, exhibited less potent antiproliferative activities than that of **D18**. With respect to amide series compounds **8a**–**8d**, introduction of aromatic heterocycles resulted in decreased antiproliferative potency relative to their parent compound **D3**, which was in line with their HDAC inhibitory activities (Table 2).

We speculated that the main reason why enhanced enzymatic inhibition of ureido series compounds did not translate into antiproliferative potency is their poor cell permeabilities and high tPSA values resulting from abundant N and O atoms; so, we designed and synthesized secondary amine series compounds with less polar atoms and lower tPSA values. In vitro activity evaluation results showed that compared with ureido compound **D18** and SAHA, the secondary amine series compounds **9a**–**9g** exhibited similar and even more potent antiproliferative activities against several tumor cell lines, although their HDAC inhibitory activities were less potent (Table 4).

Table 2 HDAC inhibitory activities of amide series compounds

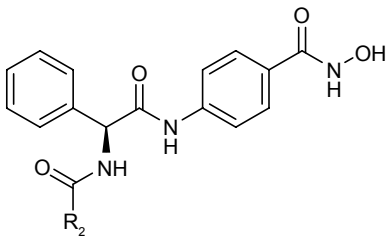

Compound	R_2	HeLa cell nuclear extract IC_{50} (nM)[a]
SAHA[b]	–	145.6
D3[b]	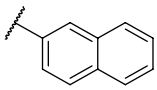	14.3
D7[b]	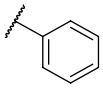	28.7
8a	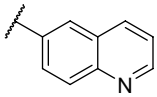	168.1
8b	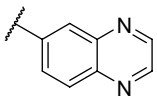	162.6
8c	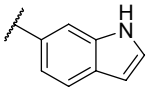	106.2
8d	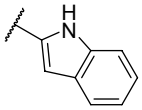	53.0
8e	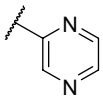	352.6

Notes: [a]Values are the mean of three experiments. The standard derivations are <20% of the mean. [b]Data from Zhang et al.[8]
Abbreviations: SAHA, suberoylanilide hydroxamic acid; IC_{50}, half-maximal inhibitory concentration; HDAC, histone deacetylase.

It was remarkable that compound **9d** was superior to **D18** and SAHA in antiproliferative evaluation against all tested tumor cell lines, including U937, U266, KG-1, HeLa, H7402, and HCT116.

Encouraged by its very potent and promising in vitro antiproliferative activity against U937 cell line (IC_{50} =0.53 μM, Table 4), we then tested the effect of compound **9d** in an in vivo U937 xenograft model with SAHA as the positive control. The tumor growth curve depicted in Figure 5 and the final tumor tissue size represented in Figure 6 explicitly showed that compound **9d** exhibited potent oral antitumor activity, which is comparable with SAHA at the same dosage of 100 mg/kg. The relative increment ratio (*T/C*) of **9d** and SAHA were 43% and 49%, respectively, both of which were significantly different from the control group ($P<0.05$) by Student's two-tailed *t*-test. Furthermore, no significant body weight loss and no evident toxic signs in macroscopic analysis of liver and spleen were detected in the mice group treated by **9d**.

Currently, most HDAC inhibitors in the clinic, including the approved drugs SAHA, PXD101, and LBH589, are the so-called pan-HDAC inhibitors with similar inhibitory activities against broad-spectrum HDACs. Similarly, our representative amide compound **D3** and ureido compound **D18** exhibited no significant selectivity among class I (HDAC1, HDAC2, HDAC3) and class IIb HDACs (HDAC6).[8] Such pan-HDAC inhibitors may be useful and acceptable in cancer treatment, but can be unacceptable and detrimental due to numerous side effects resulting from prolonged treatment of some chronic diseases such as neurologic disease and inflammatory disease. Therefore, class- or isoform-selective HDAC inhibitors with the expectation of better tolerance, fewer side effects, and broadened indications are also being developed in our lab.

Conclusion

In order to improve the antiproliferative activities of previously discovered lead compounds, 27 new L-phenylglycine-based HDAC inhibitors classified into ureido series, amide series, and secondary amine series were designed, synthesized, and evaluated. Although most of the ureido series compounds were quite effective at HDAC inhibition, their overall antiproliferative potency was disappointing. Substitution of *N*-hydroxycinnamamide for the *N*-hydroxybenzamide fragment of ureido series compounds was detrimental to their HDAC inhibitory activities. Introduction of N atoms to the amide series lead compounds got analogs with decreased enzymatic inhibition and antiproliferative potency. It is worth noting that secondary amine series compounds with less polar atoms and lower tPSA values exhibited promising

Table 3 In vitro antiproliferative activities against U937 cell line of representative ureido and amide series compounds

	Ureido series compounds								Amide series compounds				
	D18[a]	**7a**	**7b**	**7c**	**7e**	**7g**	**7h**	**7i**	**D3**[a]	**8a**	**8b**	**8c**	**8d**
U937 IC_{50} (μM)[b]	1.31	6.1	2.9	4.4	2.0	3.1	5.1	5.7	1.32	10.5	10.5	9.8	8.9

Notes: [a]Data from Zhang et al.[8] [b]Values are the mean of three experiments. The standard derivations are <20% of the mean.
Abbreviation: IC_{50}, half-maximal inhibitory concentration.

Table 4 HDAC inhibitory activities and antiproliferative activities of secondary amine series compounds

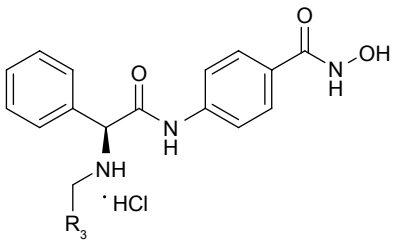

Compound	R_3	IC_{50} (nM)[a]	IC_{50} (μM)[a]					
		HeLa cell nuclear extract	U937	U266	KG-1	HeLa	H7402	HCT116
SAHA[b]	–	145.6	4.2	1.4	2.7	9.0	8.0	4.1
D18[b]	–	7.5	1.3	5.3	2.8	17.2	>20	4.0
9a	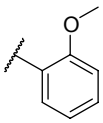	105.0	0.75	1.5	1.1	8.0	4.1	1.4
9b	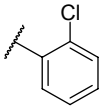	56.1	1.1	2.4	3.4	6.0	4.2	5.5
9c	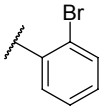	12.8	0.84	2.1	1.5	15.0	7.1	2.3
9d	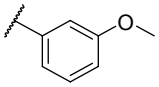	70.0	0.53	0.98	0.90	5.4	3.5	1.3
9e	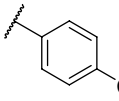	13.8	0.95	3.0	2.0	15.6	9.6	3.0
9f	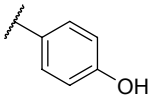	50.3	0.98	3.3	2.5	6.8	12.4	3.0
9g	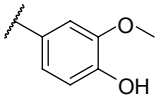	72.0	2.0	4.3	5.6	>20	>20	6.2

Notes: [a]Values are the mean of three experiments. The standard derivations are <20% of the mean. [b]Data from Zhang et al.[8]
Abbreviations: HDAC, histone deacetylase; SAHA, suberoylanilide hydroxamic acid; IC_{50}, half-maximal inhibitory concentration.

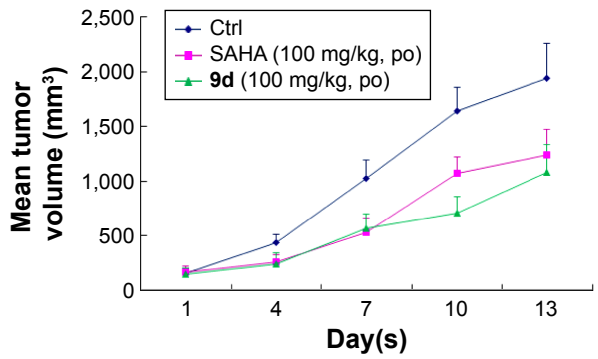

Figure 5 Growth curve of implanted U937 xenograft in nude mice.
Note: Data are expressed as the mean ± standard deviation.
Abbreviations: Ctrl, control; po, per os; SAHA, suberoylanilide hydroxamic acid.

antiproliferative activities, which indicated that poor cell permeability of ureido series compounds resulting from their higher tPSA values might be the reason for the discrepancy between enzymatic inhibition and antiproliferative potency. More importantly, at the same dosage of 100 mg/kg, secondary amine compound **9d** exhibited comparable oral antitumor activity with SAHA in a U937 xenograft model.

Acknowledgments

This work was supported by National High-tech R&D Program of China, 863 Program (Grant number: 2014AA020523), National Natural Science Foundation of China (Grant

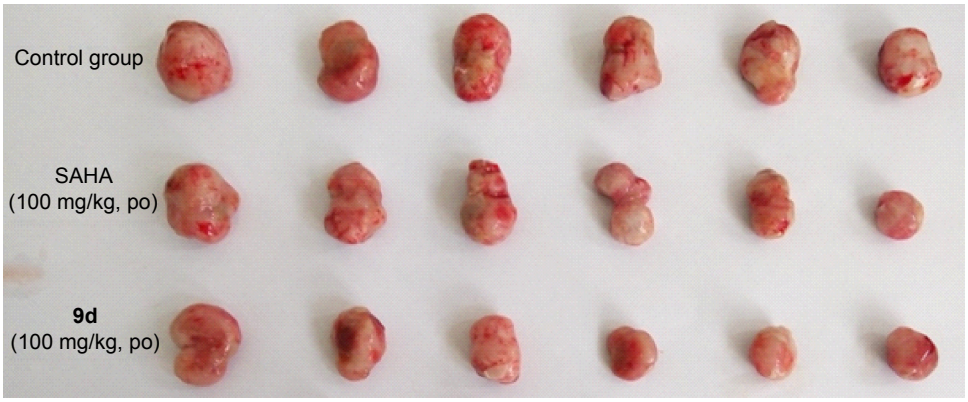

Figure 6 Picture of dissected U937 tumor tissues.
Abbreviations: po, per os; SAHA, suberoylanilide hydroxamic acid.

numbers: 21302111, 81373282, and 21172134), and China Postdoctoral Science Foundation funded project (Grant numbers: 2013M540558 and 2014T70654).

Disclosure

The authors report no conflicts of interest in this work.

References

1. Giannini G, Cabri W, Fattorusso C, Rodriquez M. Histone deacetylase inhibitors in the treatment of cancer: overview and perspectives. *Future Med Chem*. 2012;4:1439–1460.
2. Thaler F. Current trends in the development of histone deacetylase inhibitors: a review of recent patent applications. *Pharm Pat Anal*. 2012;1:75–90.
3. Gryder BE, Sodji QH, Oyelere AK. Targeted cancer therapy: giving histone deacetylase inhibitors all they need to succeed. *Future Med Chem*. 2012;4:505–524.
4. Xu WS, Parmigiani RB, Marks PA. Histone deacetylase inhibitors: molecular mechanisms of action. *Oncogene*. 2007;26:5541–5552.
5. Cea M, Cagnetta A, Gobbi M, et al. New insights into the treatment of multiple myeloma with histone deacetylase inhibitors. *Curr Pharm Des*. 2013;19:734–744.
6. Zhang L, Li M, Feng J, Fang H, Xu W. Discovery of a novel histone deacetylase 8 inhibitor by virtual screening. *Med Chem Res*. 2012;21:152–156.
7. Zhang L, Wang X, Li X, Xu W. Discovery of a series of small molecules as potent histone deacetylase inhibitors. *J Enzyme Inhib Med Chem*. 2014;29:333–337.
8. Zhang L, Zhang Y, Chou CJ, et al. Histone deacetylase inhibitors with enhanced enzymatic inhibition effects and potent in vitro and in vivo antitumor activities. *ChemMedChem*. 2014;9:638–648.
9. Ertl P, Rohde B, Selzer P. Fast calculation of molecular polar surface area as a sum of fragment-based contributions and its application to the prediction of drug transport properties. *J Med Chem*. 2000;43:3714–3717.
10. Li X, Inks ES, Li X, et al. Discovery of the first N-hydroxycinnamamide-based histone deacetylase 1/3 dual inhibitors with potent oral antitumor activity. *J Med Chem*. 2014;57:3324–3341.
11. Li X, Hou J, Li X, et al. Development of 3-hydroxycinnamamide-based HDAC inhibitors with potent in vitro and in vivo anti-tumor activity. *Eur J Med Chem*. 2015;89:628–637.
12. Duan W, Li J, Inks ES, et al. Design, synthesis and antitumor evaluation of novel histone deacetylase (HDAC) inhibitors equipped with phenylsulfonylfuroxan module as nitric oxide (NO) donor. *J Med Chem*. 2015;89:4325–4338.